Cerebral Cortex, April 2018;28: 1297–1311

doi: 10.1093/cercor/bhx043
Advance Access Publication Date: 25 February 2017
Original Article

ORIGINAL ARTICLE

Attenuated Fast Steady-State Visual Evoked Potentials During Human Sleep

Omer Sharon[1,2] and Yuval Nir[1,2,3]

[1]Sagol School of Neuroscience, Tel Aviv University, Tel Aviv 69978, Israel, [2]Department of Physiology and Pharmacology, Sackler School of Medicine, Tel Aviv University, Tel Aviv 69978, Israel and [3]Functional Neurophysiology and Sleep Research Lab, Tel-Aviv Sourasky Medical Center, Tel Aviv 64239, Israel

Address correspondence to Yuval Nir, Sagol School of Neuroscience, Department of Physiology and Pharmacology, Sackler School of Medicine, Tel Aviv University, Tel Aviv 69978, Israel. Email: ynir@post.tau.ac.il

Abstract

During sleep, external sensory events rarely elicit a behavioral response or affect perception. However, how sensory processing differs between wakefulness and sleep remains unclear. A major difficulty in this field stems from using brief auditory stimuli that often trigger nonspecific high-amplitude "K-complex" responses and complicate interpretation. To overcome this challenge, here we delivered periodic visual flicker stimulation across sleep and wakefulness while recording high-density electroencephalography (EEG) in humans. We found that onset responses can be separated from frequency-specific steady-state visual evoked potentials (SSVEPs) selectively observed over visual cortex. Sustained SSVEPs in response to fast (8/10 Hz) stimulation are substantially stronger in wakefulness than in both nonrapid eye movement (NREM) and REM sleep, whereas SSVEP responses to slow (3/5 Hz) stimulation are stronger in both NREM and REM sleep than in wakefulness. Despite wake-like spontaneous activity, responses in REM sleep were similar to those in NREM sleep and different than wakefulness, in accordance with perceptual disconnection during REM sleep. Finally, analysis of amplitude and phase in single trials revealed that stronger fast SSVEPs in wakefulness are driven by more consistent phase locking and increased induced power. These results suggest that the sleeping brain is unable to effectively synchronize large neuronal populations in response to rapid sensory stimulation.

Key words: EEG, NREM sleep, REM sleep, sensory, SSVEP

Introduction

Sleep is defined as reversible disconnection from the environment—a state where external sensory stimuli rarely affect perceptual awareness or elicit a meaningful behavioral response, unless they are strong enough to cause an awakening (Nir and Tononi 2010). Disconnecting from the outside world during sleep is dangerous, yet all animals carefully investigated show forms of sleep (Cirelli and Tononi 2008). In some cases, such as unihemispheric sleep in dolphins (Mukhametov et al. 1977), animals developed remarkable specializations enabling safe disconnection rather than eliminating sleep altogether, suggesting that sleep serves an essential function that cannot be achieved while interacting with the external world. Whatever this function may be (e.g., synaptic downscaling (Tononi and Cirelli 2014), memory consolidation (Marshall and Born 2007), brain restoration (Xie et al. 2013), or other) it seems that associated processes are not compatible with full-blown processing of external sensory inputs. Therefore, elements of sensory responses that are absent during sleep may point to important differences in brain activity that are required to support sleep function.

During nonrapid eye movement (NREM) sleep, neuronal activity is dramatically different (Steriade et al. 2001) so disconnection from the outside world may not be entirely surprising. Hyperpolarized neurons throughout the thalamus and the cortex exhibit bistable activity and stereotypical oscillations

(Steriade et al. 2001). When this cellular bistability occurs in-phase across multiple brain regions, it gives rise to high-amplitude slow waves in scalp electroencephalography (EEG) (>70 μV, 0.5–4 Hz). Importantly, even when scalp EEG only shows modest slow wave activity, this often reflects slow waves occurring out-of-phase across different regions (Nir et al. 2011), so the underlying neuronal activity remains disrupted and qualitatively different than in wakefulness, in line with changes in consciousness (Nir et al. 2013). However, disconnection persists also during REM sleep, despite its wake-like "activated" EEG (Nir and Tononi 2010), which remains mysterious.

Despite disconnection from external stimuli, it is also clear that discriminative sensory processing persists during sleep to some degree. Behaviorally relevant stimuli, such as hearing one's name, lead to more frequent awakenings (Oswald et al. 1960; McDonald et al. 1975) and induce a spread of cortical activation (Portas et al. 2000). Late event-related potentials (ERPs) during sleep are observed in response to semantically incongruous words (Bastuji et al. 2002) and in response to stimuli associated with a previously learned task (Kouider et al. 2014). Thus, at least in the auditory domain, sensory processing during sleep is extensive and complex while at the same time sounds rarely lead to explicit recollection, meaningful behavioral response, or perception. Thus, it remains unclear precisely how sensory processing during sleep differs from the response patterns during wakefulness.

Early comparisons of sensory responses in wakefulness and sleep argued for "thalamic gating" (Steriade et al. 1993), whereby responses in NREM sleep are attenuated at thalamic relay nuclei and primary sensory cortices (Evarts 1963; Mukhametov and Rizzolatti 1970; Gucer 1979; Livingstone and Hubel 1981; Mariotti et al. 1989; Edeline et al. 2001). However, more recent studies—especially in the auditory domain—found preserved activation of primary sensory cortices (Pena et al. 1999; Portas et al. 2000; Issa and Wang 2008; Riedner et al. 2011; Nir et al. 2015). Some studies report stronger responses in sleep and anesthesia compared with wakefulness (Kakigi et al. 2003; Imas et al. 2005).

A central challenge is that brief sensory stimuli presented during NREM sleep often produce a K-complex, a huge (>70 μV) EEG event that can be evoked by an external stimulus yet can also appear spontaneously, and its function remains a subject of ongoing debate—with suggestions ranging from arousal to sleep protection (Colrain 2005). The late components of the K-complex waveform are largely nonspecific (i.e., very similar in appearance regardless of the precise sensory event that triggered it), making it difficult to reliably isolate selective sensory responses (Perrin et al. 2000; Colrain and Campbell 2007; Laurino et al. 2014).

Therefore, we sought to develop a noninvasive method that goes beyond existing limitations of sleep EEG studies and allows a novel comparison of sensory responses across wakefulness and sleep: (1) one that produces strong responses in sensory regions that are easily accessible with scalp EEG (such as visual cortex), (2) one that elicits robust responses without the need for participants to actively perform a task—so that differences between wakefulness and sleep do not simply reflect passive processing, (3) one that rarely leads to awakenings, and most importantly, and (4) one that overcomes the challenge of K-complexes. We chose periodic sensory stimulation that drives steady-state evoked potentials (SSEP) (Regan 1966), since such paradigms were shown to be effective in the visual (Norcia et al. 2015), auditory (Galambos et al. 1981; Tlumak et al. 2012) and somatosensory (Colon et al. 2012) modalities. Moreover, steady-state stimulation offers superior signal-to-noise ratio (SNR), since EEG noise and artifacts are mostly broadband while the response is narrowband. In addition, steady-state visual evoked potential (SSVEP) shows minimal adaptation to repeated stimulation (Regan 1966), which is key when stimulating repeatedly throughout the night. Lastly, auditory SSEPs have been shown to correlate with perceptual awareness (Galambos et al. 1981) and to be modulated by sleep (Llinas and Ribary 1993) and anesthesia (Plourde 2006).

We thus set out to harness steady-state visual stimulation to study how sensory responses differ between wakefulness and sleep states. We anticipated that this method may allow to go beyond onset and nonspecific responses to study selective sensory responses across states. Moreover, we hypothesized that selective sensory responses during both NREM and REM sleep will be similar, and different than those in wakefulness, mirroring the differences in perception and behavior.

Materials and Methods

Participants

Full-night sleep recordings were performed in 20 healthy young adults (mean age: 28.0 ± 0.83 years, range: 22–35, 11 females). Written informed consent was obtained from each participant. The study was approved by the Medical Institutional Review Board at the Tel Aviv Sourasky Medical Center. Participants reported to be healthy, without any history of neuropsychiatric or sleep disorders. Data from one participant was excluded from further analysis due to technical problems in stimulus presentation, 19 participants remained after this exclusion (mean age: 28.1 ± 0.81, 11 females).

Sleep Recordings and Experimental Design

Participants arrived at the lab around midnight (and slept until late morning to in order maximize the occurrence of REM sleep) and after EEG setup and receiving instructions (e.g., to keep eyes closed throughout the study) proceeded to sleep. High-density EEG was continuously recorded (details below) along with electrooculogram (EOG) and electromyogram (EMG) across an entire night of sleep. All recordings were performed in a dark, acoustically attenuated and electrically shielded sleep lab. First, participants were asked to stay awake while lying down with closed eyes in bed as we ran one block of visual stimulation (either 200 trials [$n = 16$] or 160 trials [$n = 3$], roughly 35 min). Participants were woken up immediately upon any signs of falling asleep such as rolling eye movements, EEG slowing, or appearance of sleep spindles or K-complexes. After stimulation during wakefulness, participants were left to sleep undisturbed and were instructed to keep their eyes closed throughout the study. Upon waking up in the morning, most participants (18/19) were asked to remain with closed eyes, lying down, as we acquired an additional block of trials during consolidated wakefulness.

Visual Stimulation

Visual stimuli were delivered using custom-made "ski-like" goggles (Fig. 1E) tiled with 88 light-emitting diodes (LEDs, Adafruit) placed roughly 4 cm from the eyes. Light illumination in the LEDs was controlled using Arduino Mega (Arduino) directed by Matlab (The Mathworks) on a personal computer. Before using the device in experiments, we first verified that activating the LEDs did not induce any electrical artifacts in a mock setup

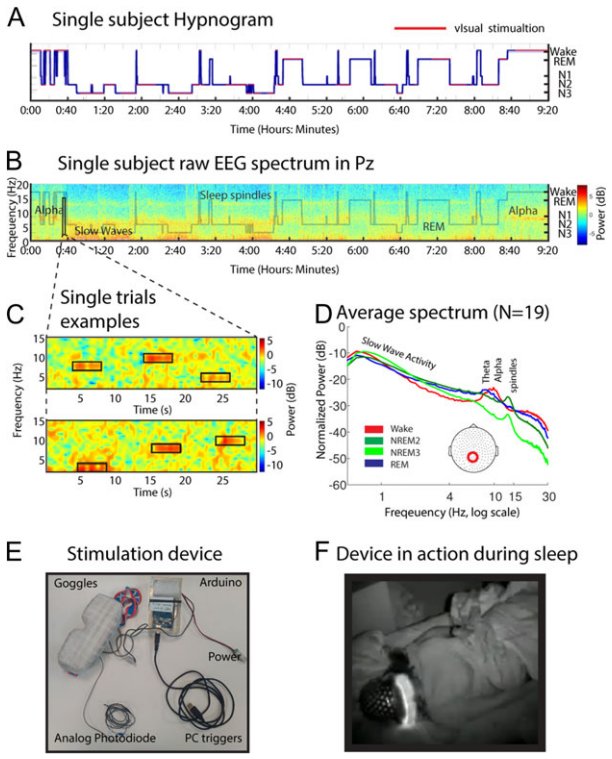

Figure 1. Experimental setup and sleep properties during overnight visual stimulation. (*A*) Representative hypnogram. Red, visual stimulation trials. (*B*) Representative time–frequency representation of scalp EEG (Pz) recorded in one individual (same subject as (*A*)) during a full-night sleep study. Warm colors (e.g. red) mark increased power in specific time–frequency windows (frequency shown on left side of *y*-axis). Superimposed hypnogram (gray trace) marks the time-course of sleep/wake states (shown on right side of *y*-axis). Note that wakefulness is associated with increased power in the alpha (8–12 Hz) range, nonrapid eye movement (NREM) stages N2 and N3 are associated with increased power in spindle (10–15 Hz) and slow (<4 Hz) frequency ranges, respectively, while REM-sleep exhibits diffuse theta (6–9 Hz) activity. (*C*) Representative time–frequency representation of scalp EEG (Oz) acquired during 30 s of wakefulness shows single-trial responses to visual stimulation at 8, 10, 5 Hz (upper example) and 3, 8, 10 Hz (lower example). (*D*) Mean EEG power spectrum (around Pz, inset) across different states of wakefulness and sleep ($n = 19$ participants). Red, wake; dark green, N2; light green, N3; Blue, REM sleep. Note that wakefulness is characterized by increased power in alpha (8–12 Hz) and high (>20 Hz) frequencies, NREM sleep is associated with increased power in slow (<4 Hz) and spindle (10–15 Hz) frequencies, while increased theta (6–9 Hz) activity accompanies REM sleep. (*E*) Visual stimulation device consisted of custom-made goggles ("Goggles") densely tiled with LEDs (Methods) controlled by a PC and Arduino interface ("Arduino"). An analog photodiode ("Analog Photodiode") embedded within the goggles allowed light measurements during experiments, and the precise timing of stimuli was synchronized with EEG measurements ("PC triggers"). (*F*) video example of 13 s visual stimulation during sleep, see Supplementary movie 1.

where EEG was recorded from a melon (Fig. S1). Average luminance at the approximate eye locations was 2.5 cd/m^2, as measured with Minolta luminance meter LS-110. Light stimulation was dominated by red wavelengths (its amplitude spectrum peaked at 600 nm), as measured with Thorlabs CC S100 spectrometer (Fig. S2). An analog photodiode was placed inside the goggles in order to record the actual emitted light online during experiments, synchronized and stored along with the EEG data. In each 4-s trial, light intensity was modulated sinusoidally across all LEDs simultaneously at a specific frequency (either 3, 5, 8, or 10 Hz, Fig. S2). These frequencies were chosen (1) based on a pilot study assessing the effectiveness of a wide range of stimulation frequencies (not shown), and (2) since they represent classical frequency bands of interest (delta, delta/theta, theta, and alpha). Given that previous studies reported that attention enhances second harmonic responses (Kim et al. 2011), we used sinusoidal stimuli (rather than on/off box-car stimuli) to ensure that any harmonics in brain activity cannot be attributed to harmonics in the stimulus itself. Intertrial intervals were pseudorandom between 4 and 6 s (with jitter) to avoid expectation effects (example in Fig. 1C). Each block consisted of either 200 trials (16 participants) or 160 trials (3 participants) and was initiated manually by the experimenter. Typically, during a full night we ran 5–10 blocks, each with 40–50 trials for each frequency.

Data Acquisition

High-density EEG was recorded continuously using a 256-channel hydrocel geodesic sensor net (Electrical Geodesics, Inc. system [EGI]). Each carbon-fiber electrode consists of a silver-chloride carbon fiber pellet, a lead wire, a gold-plated pin, and was injected with conductive gel (Electro-Cap International). Signals were referenced to Cz, amplified via an AC-coupled high-input impedance amplifier (NetAmps 300, EGI), and digitized at 1000 Hz. Electrode impedance in all sensors was verified to be <50 kΩ before starting the recording. EEG was band-pass filtered offline between 0.5 Hz and 45 Hz, and an additional notch filter at 50 Hz was further applied to the continuous data offline to remove residual line noise using a Kaiser type finite impulse response filter with zero phase shift

Sleep Scoring

Manual sleep scoring was performed according to established guidelines of the American Academy of Sleep Medicine (Iber et al. 2007). EEG data from F3/F4, C3/C4, and O1/O2 were re-referenced to a mastoid in the contralateral hemisphere, EOG from E1/E2 were referenced to the other Mastoid, and these were visualized in 30 s epochs together with synchronized EMG. Successful scoring was further verified by inspecting the time–frequency representation (spectrogram) of the Pz electrode (not involved in scoring process) superimposed with the hypnogram (as in Fig. 1B). N1 epochs (28 min per participant on average, range: 11–58 min) were excluded from further analysis to avoid uncertainty regarding precise sleep onset and participant state. Each participant was debriefed in the morning regarding her sleep quality, dreams, or any other experiences during the night. Each trial was categorized according to the sleep stage it occurred in (W/N1/N2/N3/REM) and analysis was performed separately according to this categorization. W (wakefulness) trials include the first and last blocks with continuous wakefulness, as well as intermittent epochs during the night.

EEG Preprocessing

EEG processing was performed in MATLAB (The MathWorks) using custom-written scripts as well as functions from the FieldTrip toolbox (Oostenveld et al. 2011). Data were first down-sampled to 250 Hz and was then divided into 12 s segments, taking 4 s before and 8 s after the onset of each stimulus. The 12 s epochs were linearly de-trended, and baselined-corrected to the average voltage in the interval [−4 s -> −1 s] before stimulation onset. Bad channels (<8% in all participants) were identified as those electrodes whose variance and maximal absolute

value constituted outliers relative to adjacent electrodes upon visual inspection per participant, and were interpolated using a linear, distance weighted interpolation. Artifact trials (<10% in all participants) were identified as those epochs whose variance and maximal absolute value constituted outliers relative to all trials, and were discarded from subsequent analysis. Next, the data were re-referenced to the average potential across all electrodes (average reference). After these steps, we only considered data for a specific condition (specific frequency × specific state) whenever at least 20 repetitions of that condition were available for analysis in a given participant. We also verified that subjects did not open their eyes during wakefulness blocks, by inspecting the vertical EOG derivative (difference between electrodes located just below and just above the eye orbit). Only 1.1 ± 0.4% of the trials per subject were associated with brief eyes opening.

Analysis of Average Visual-Evoked Activity

ERPs evoked by the visual stimuli (Fig. 2) were characterized as follows. EEG data were taken from a predefined region of interest (ROI) consisting of 10 electrodes surrounding Oz over the

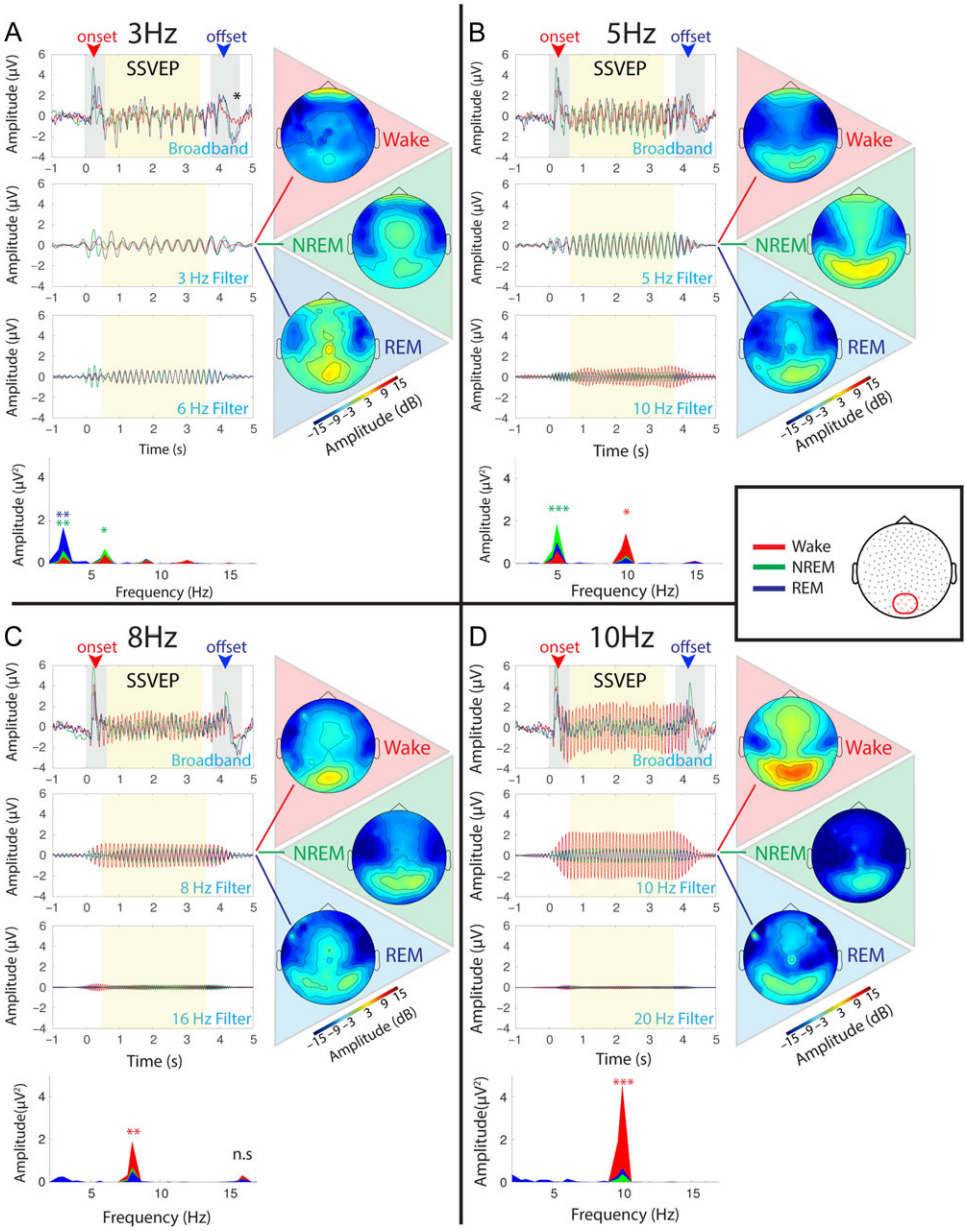

Figure 2. Visually evoked EEG responses across wakefulness and sleep. (*A*) EEG responses (grand mean, averaged across trials and then across participants) from a region of interest around Oz over occipital cortex (inset, right) in response to sinusoidal visual stimulation at 3 Hz. Left column, rows (top to bottom) depict broadband signal (top), EEG band-pass filtered around the stimulation frequency (middle), and the second harmonic (bottom). Gray and yellow regions mark periods of onset and steady-state responses, respectively. Red arrow marks onset response and blue the positive offset while a black asterisk shows the negative offset. Right column, scalp topography of steady-state visual response in wakefulness (red, top), NREM sleep (green, middle) and REM sleep (blue, bottom). Bottom inset shows the power spectral density of the steady-state response in wakefulness (red), NREM sleep (green) and REM sleep (blue). (*B*) Same format for visual stimulation at 5 Hz. (*C*) Same format for visual stimulation at 8 Hz. (*D*) Same format for visual stimulation at 10 Hz. Note that during wakefulness, visual stimulation at 8/10 Hz entrains the EEG response more strongly.

occipital lobe (see ROI inset in Fig. 2). The 12 s data in this ROI around each trial were first averaged across electrodes for each condition (frequency * state), then averaged across trials, and finally averaged across participants. For visualization purposes, these averaged ERPs (Fig. 2, top rows) were high-pass filtered above 0.5 Hz (second order Butterworth filter) to remove residual DC/ultra-slow waves in the average waveforms. In addition, the averaged data were band-passed filtered (second order Butterworth filter) at ±1 Hz around the stimulation frequency (Fig. 2, middle rows) and at ±1 Hz around the second harmonic of the stimulation frequency (Fig. 2, bottom rows) to further evaluate the extent of EEG entrainment by the visual stimuli. To compare the responses to identical visual flicker across frequencies and states, we analyzed separately trials occurring during wakefulness, NREM sleep, and REM sleep (Fig. 2). We first considered N2 and N3 separately but all results were nearly identical. Therefore, examination of EEG in these states was collapsed throughout subsequent analysis. We also compared responses in early NREM sleep (first half of NREM trials) with those in late NREM sleep (second half of NREM trials), but did not find significant differences ($P > 0.38$ for all comparisons, see Fig. S3).

Onset responses were calculated as the maximal voltage 0–0.5 s post stimulus onset and offset responses were differentiated to two components: an early positive deflection (blue arrow in Fig. 2A upper panel, calculated as the maximal voltage 0–0.3 s post stimulus offset), and a late negative component (black asterisk in Fig. 2A upper panel, calculated as the minimal voltage 0–1 s post stimulation offset). To check whether the onset/offset response varied as a function of stimulation frequency and state, we used a 2-way ANOVA to verify there was no interaction. Given that there was no interaction, we averaged onset/offset responses across frequencies, and proceeded to compare those across states via paired permutation tests (as in all subsequence analysis, see Permutation-Based Testing section).

We also examined to what extent visual stimulation was associated with K-complexes. To this end, we detected K-complexes as in previous studies (Riedner et al. 2007; Nir et al. 2011). Briefly, K-complexes were detected by band-pass filtering the EEG signal in Pz electrode between 0.5 and 4 Hz (second order Butterworth filter). The first-order derivative was used to detect local extrema and identify individual waves. Individual slow waves with peak-to-peak amplitude exceeding 75 μV, a duration of 0.5–2 s, and isolated from other slow waves by at least 3 s were considered as K-complexes. We then quantified the occurrence of K-complex positive peaks around stimulus presentation in each state (Fig. S4).

EEG power was computed for the steady-state response component (0.5–3.5 s following stimulus onset, see dark gray areas in Fig. 2) via the Fast Fourier Transform (FFT) after multiplying by a hamming window, yielding a frequency resolution of 0.33 Hz. The power spectrum of the baseline (average of all intervals [−4 s -> −1 s] before stimulus onset) was subtracted from the evoked power spectrum of the stimulation period for each participant and channel separately. These "difference" spectra (stimulation-baseline) were averaged and displayed (Fig. 2 lowermost panels), used for visualization of scalp topographies, and used for statistical testing ($n = 19$ in wake vs. NREM sleep; $n = 10$ in wake vs. REM sleep). Scalp topography of EEG power is shown with color-coding, where the color of each scalp sensor represents the EEG power at the stimulation frequency (dB scale). In order to verify that signals were stable throughout long full-night recordings, we compared ERPs in morning wakefulness and evening wakefulness data and verified they did not exhibit significant differences (Fig. S5).

Analysis of Single-Trial Visual-Evoked Activity

The EEG response in individual trials was extracted from the same occipital ROI during the steady-state response component (0.5–3.5 s following stimulus onset) and transformed into the frequency domain via FFT. In addition, a matched baseline interval [−4 s -> −1 s] before stimulus onset was extracted. For each trial/baseline interval, we extracted the amplitude (absolute value of the FFT coefficient) and phase (the angle of the complex FFT coefficient) at the stimulation frequency. Such analysis (Fig. 4) allows separating amplitude and phase contributions to the EEG response at the single-trial level. For each state (wake/NREM/REM) and frequency (3/5/8/10 Hz) we computed the distribution of phase and amplitude values (as percent of total power) and expressed them as a normalized histograms depicting the probability of occurrence (area = 1). Phase distributions (Fig. 4, bottom rows) were plotted on a circular graph ("rose plot"), while amplitude distributions (Fig. 4, top rows) were plotted as regular histograms. Average phase and amplitude values across trials for each participant (tick marks in Fig. 4 upper rows, one value per participant) were then used for random-effect statistics. To test for potential phase differences that change as a function of vigilance state, circular phase distributions were first computed for each participant (circles in Fig. 4 lower rows), and then a paired random-effect permutation test was performed (as described below) this time replacing regular mean and difference functions with circular mean and circular difference functions as implemented in "CircStats" toolbox for MATLAB (Berens 2009).

Consistency of phase (phase coherence) was quantified using phase locking value (PLV) as implemented in "CircStats" toolbox for MATLAB (Berens 2009):

$$\mathrm{ITPC} = \frac{1}{N}\sum_{k=1}^{N} e^{i * \phi_k}$$

$$\mathrm{PLV} = |\mathrm{ITPC}|$$

where N signifies the number of trials and ϕ_k denotes the phase of the spectral estimate of trial k at the stimulation frequency. ITPC is a measure ranging from 0 to 1, where a value of one signifies perfect synchronization of phases between trials and a value of 0 signifies a complete desynchronization of phases (however, for a finite N, the average ITPC for a uniform phase distribution is always >0). We evaluated PLV across participants (Fig. 4), as well as phase coherence across trials within each participant, via a permutation test (in this context, we focused on trials with sufficiently strong response at the stimulation frequency relative to immediately preceding baseline—upper 75% of trials) to avoid contamination by trials without significant difference from baseline (Fig. 4, upper panels).

Visual-Evoked Potential Waveforms and Topography

Visual-evoked potential (VEP) waveforms were averaged across stimulation cycles to generate a "standard ERP" in response to each light transient (Fig. 5). "Time zero" for averaging was defined as the maximal actual luminance recorded online by the photodiode. Each cycle was created by averaging consecutive time intervals in the grand-average ERP (across participants). We especially wanted to investigate the topography of

phase differences observed in Figure 4, so topographies were created every 16 ms in ±4 time points in relation to maximal light—"time-zero".

Comparison of Evoked and Spontaneous Oscillations

In order to assess a possible relationship between the evoked response in 8/10 Hz and spontaneous alpha rhythm, we extracted the entire EEG time-course from the occipital ROI when visual stimuli were not delivered during wakefulness (when alpha is classically defined). These epochs were concatenated and transformed to the spectral domain using FFT (as above). For each participant we extracted (1) the dominant alpha frequency, defined as the frequency with maximal amplitude between 8 and 12 Hz, and (2) the amplitude at that frequency. We then calculated, in each participant, the Pearson correlation between these measures and the strength of the evoked response at 8/10 Hz for the same participant (same values whose average is shown in Fig. 2 lower panels). In order to address the same question regarding low frequencies, we repeated the exact same analysis for evoked power in 3/5 Hz and correlated it with spontaneous EEG power in the slow frequency range 0.1–5 Hz during NREM sleep in nonstimulated epochs. In the alpha range we also tested whether participants with slower (vs. faster) spontaneous alpha activity could predict preferred response to 8 (vs. 10 Hz) stimulation. To this end, we calculated the correlation between each participant's dominant (peak) frequency and the participant preferred response frequency in response to 8/10 Hz, computed the distance of the dominant spontaneous frequency from the frequency of response to 8/10 Hz stimulation, and correlated this distance with the amplitude of the evoked response.

Statistical Analysis

Error bars throughout the manuscript denote standard error of the mean (SEM = SD/$\sqrt{[n-1]}$). Given our predefined ROI (a single continuous scalp region composed of the average signal across 10 electrodes) we did not correct for multiple comparisons across sensors. For hypothesis testing we used a nonparametric permutation test in a random effects approach (first extracting one value of interest per participant, then testing real effects in relation to permutated labels). As discussed in Maris and Oostenveld (2007), this straight-forward intuitive procedure does not make any assumptions regarding the origin distribution. Nevertheless, we verified that all results were also significant when using ANOVA (less stringent, not shown).

Permutation-Based Testing

We used random paired permutation tests in the context of 22 different comparisons across states: (tests #1–8) amplitude of steady-state responses at each frequency and its harmonic separately (3, 5, 8, 10 Hz and 6, 10, 16, 20 Hz), (tests #9–16) phase of steady-state responses at each frequency and its harmonic separately (3, 5, 8, 10 Hz and 6, 10, 16, 20 Hz), (test #17) latency of onset responses (collapsed across all frequencies), (test #18) amplitude of onset responses (collapsed across all frequencies), (test #19) latency of positive offset responses (collapsed across all frequencies), (test #20) latency of negative offset responses (collapsed across all frequencies), (test #21) amplitude of positive offset responses (collapsed across all frequencies), (test #22) amplitude of negative offset responses (collapsed across all frequencies).

The dependent variable in each one of these 22 tests was compared in a pair-wise manner across the different stages (wake vs. NREM; wake vs. REM, NREM vs. REM) using random paired permutation as follows: for each paired comparison (e.g., wakefulness steady-state 8 Hz amplitude vs. REM-sleep steady-state 8 Hz amplitude in 10 participants), the mean value (averaged across trials for each participant separately) was compared such that the correct labels (wake / REM) were either swapped or not-swapped randomly (e.g., 2^{10} permutations for 10 participants). The same procedure was performed for wakefulness versus NREM sleep (2^{19} permutations for 19 participants), as well as NREM sleep versus REM sleep (2^{10} permutations). Results were considered significant only if the experimental observation was in the upper/lower 2.5% tail, after correcting the critical *P*-values for multiple comparisons using the False Discovery Rate (FDR) (Benjamini and Yekutieli 2011). Such correction was applied for all tests, given that each test entailed multiple pair-wise comparisons (e.g., when comparing SSVEP amplitude across 3 state pairs * 4 frequencies * 2 harmonics).

Results

To investigate state-dependent sensory processing in humans, we compared responses to visual stimulation across wakefulness and sleep states by performing full-night sleep studies with high-density EEG while intermittently delivering periodic visual flicker stimulation through custom goggles and closed eyes (Fig. 1*E*). Continuous overnight sleep studies were conducted in healthy young adults (n = 19) with polysomnography including EOG, EMG, scalp EEG, and video monitoring. Visual stimuli lasted 4 s, during which luminance was modulated sinusoidally at one of several frequencies (3, 5, 8, 10 Hz), allowing to examine separately the effects of wakefulness and sleep on onset/offset responses versus SSVEPs.

Normal Sleep is Preserved With Intermittent Visual Stimulation

Continuous overnight recordings lasted 8 h and 20 min on average (±11 min). All participants completed one block of visual stimulation while awake (about 40 min, see Methods), were then left to sleep undisturbed, and 18/19 participants completed an additional visual stimulation block in the morning upon awakening. Sleep was scored in 30 s intervals according to established guidelines (Iber et al. 2007). Sleep EEG showed all the established hallmarks of the different vigilance states (Fig. 1*B*), including alpha (8–10 Hz) activity during quiet wakefulness, sleep spindle (10–15 Hz) sigma activity during N2 sleep, slow wave (<4 Hz) activity during N3 sleep, and diffuse theta (6–9 Hz) during REM sleep. Moreover, the mean power spectrum of the scalp EEG across all participants revealed these spectral signatures across the entire group (Fig. 1*D*). We did not observe any awakenings associated with visual stimulation (and even if rare awakenings were present and not observed, this would cause sleep trials to be tagged as wake, so any differences reported here would constitute a lower bound). In addition, sleep parameters (e.g., sleep efficiency, sleep latency, wake after sleep onset, as well as the percentage of specific stages out of total sleep time) were in accordance with typical values for healthy young adults (Table 1) (Carskadon and Dement 2005). Debriefing the participants in the morning, all participants reported that they were not aware if (cannot recall whether) stimuli were being presented after they had gone to sleep, and

Table 1 Overnight sleep measures

Total time in bed (min)	435.59 ± 10.9
Total sleep time (min)	373.48 ± 13.6
Sleep efficiency (%)	86.38 ± 3.2
Sleep latency, (min)	14.1 ± 5.5
WASO (%)	15.4 ± 4.6
Stage 1 (%)	6.81 ± 0.9
Stage 2 (%)	55 ± 1.7
SWS (%)	24.83 ± 1.6
NREM (%)	86.65 ± 2
REM (%)	13.35 ± 2

Average overnight sleep measures expressed as mean ± SEM ($n = 19$). Percentage values are expressed per total sleep time, excluding blocks of forced wakefulness. Sleep efficiency corresponds to total sleep time per time in bed. Sleep latency is to Stage 2. WASO refers to waking after sleep onset; SWS, slow-wave sleep; NREM, nonrapid eye movement; REM, rapid eye movement. Note that sleep measures indicate sleep was largely normal for a first night in a sleep lab.

all participants reported being well-rested (slept very well, not tired). Thus, intermittent visual stimulation did not exert observable effects on sleep architecture or subjective measures and may be less disruptive than sensory stimulation in other modalities (e.g., auditory) where it can commonly lead to awakenings, sleep fragmentation, and attenuated slow wave activity (Landsness et al. 2009).

Periodic Visual Flicker Stimulation Through Closed Eyes Effectively Entrains Visual Responses

EEG responses to visual flicker were first examined using a classical evoked ERP averaging analysis (Fig. 2). We focused our analysis on an occipital ROI defined a priori (Methods). For all frequencies and vigilance states, the EEG response was specific to the stimulation frequency and its second harmonic (power spectra, Fig. 2), and was maximal at occipital electrodes (scalp topographies, Fig. 2). This established that full-field visual flicker through closed eyes in the absence of an explicit task was nevertheless highly effective in driving robust responses across states of wakefulness and sleep. In fact, the SNR of EEG responses to the periodic stimuli revealed frequency-specific responses in individual trials (Fig. 1C). The average ERPs in response to all stimulation frequencies (upper traces, Fig. 2) consisted of an initial large positive component (in an amplitude range of 4.3–8.7 μV, gray highlight, red arrows) following stimulus onset (220–240 ms). The onset response was followed by a near-sinusoidal SSVEP at the stimulation frequency (yellow highlight). Following stimulus termination, an offset response appeared in sleep, consisting of a positive onset-like deflection (2.5–3 μV), followed by a prolonged negativity lasting several hundred milliseconds (−2.5 μV in the peak, gray highlight blue arrows, Fig. 2).

Onset Responses are Stronger in NREM Sleep, Offset Responses Appear Only in Sleep

The onset response was maximal in NREM sleep (5.9 ± 0.46 μV) and significantly stronger than during wakefulness (4.25 ± 0.34 μV, $P = 10^{-6}$, FDR corrected) in line with previous findings (Okusa and Kakigi 2002; Massimini et al. 2007; Harris and Thiele 2011; Laurino et al. 2014; Nir et al. 2015). Onset responses in REM sleep were similar in magnitude to those during wakefulness (4.34 ± 0.44 μV, $P = 0.019$, not significant after FDR correction) and lower than NREM sleep ($P = 0.004$ FDR corrected). In the vast majority of trials (99%) steady-state visual stimulation did not elicit K-complexes, nor was the distribution of sporadic K-complex events around stimulus presentation locked to specific temporal intervals (Fig. S4).

Offset responses consisted of a positive "onset-like" deflection (blue arrow in Fig. 2A upper panel) observed during sleep (90–200 ms post stimulus termination), whose amplitude was comparable in NREM sleep (2.96 ± 0.22 μV) and in REM sleep (2.51 ± 0.19 μV, $P = 0.11$), but significantly stronger than during wakefulness (2.13 ± 0.20 μV, $P = 0.001$, FDR corrected for NREM but only trending for REM, $P = 0.028$). Following this positive peak, a prolonged negative deflection (black asterisk in Fig. 2A upper panel) appeared much stronger in NREM (−2.55 ± 0.23 μV) and REM sleep (−2.47 ± 0.15 μV) compared with wake (−1.63 ± 0.11 μV, $P = 10^{-5}$ and 10^{-4} for NREM and REM sleep, respectively, both FDR corrected) and its amplitude was comparable across NREM and REM sleep ($P = 0.24$). Overall, onset and offset responses exhibited an occipital (visual) topography, although the diffuse negative offset response appeared to include more anterior parietal regions and might constitute a nonspecific response (Amzica and Steriade 2002; Colrain and Campbell 2007; Pigarev et al. 2011), see also Discussion.

SSVEP to 8/10 Hz Visual Flicker are Stronger in Wakefulness While Responses to 3/5 Hz Stimulation are Stronger in Sleep

After the initial onset response, the EEG exhibited robust SSVEPs and we set out to compare in detail these SSVEPs across states for each stimulation frequency (Fig. 2, middle rows) and its second harmonic (Fig. 2, lower rows). Generally, analysis of the SSVEP power spectrum (Fig. 2, bottom panels) confirmed that SSVEPs were highly robust, specific to the stimulation frequency (and apparent to a lesser extent in the second harmonic), and that wakefulness was associated with stronger SSVEPs in response to 8/10 Hz stimulation in contrast to sleep states that were associated with stronger response to 3/5 Hz stimulation.

At the lowest stimulation frequency (3 Hz), the magnitude of the SSVEP was maximal in REM sleep (1.71 ± 0.56 μV^2) and significantly stronger than that observed in wake (0.3 ± 0.07 μV^2, $P = 5 * 10^{-4}$, FDR corrected) and in NREM sleep (0.6 ± 0.14 μV^2, $P = 0.008$, FDR corrected). SSVEP to 3 Hz in NREM was also significantly stronger than wake ($P = 0.009$, FDR corrected). In response to 5 Hz stimulation, the magnitude of the SSVEP was maximal in NREM sleep (1.86 ± 0.44 μV^2) and significantly larger than that during wake (0.59 ± 0.12 μV^2, $P = 2 * 10^{-4}$, FDR corrected) and REM sleep (0.99 ± 0.43 μV^2, $P = 7 * 10^{-4}$, FDR corrected), while the response in REM was not significantly different than that during wakefulness ($P = 0.27$).

In contrast, in response to 8/10 Hz stimulation, the SSVEP was significantly stronger in wakefulness (8 Hz: 1.91 ± 0.12 μV^2; 10 Hz: 4.57 ± 0.1 μV^2) when compared with both NREM sleep (8 Hz: 0.67 ± 0.18 μV^2, $P = 10^{-3}$; 10 Hz: 0.37 ± 0.09 μV^2, $P = 10^{-4}$, both FDR corrected) and REM sleep (8 Hz: 0.5 ± 0.12 μV^2, $P = 0.009$; 10 Hz: 0.001 ± 0.21 μV^2, $P = 0.001$, both FDR corrected) and not significantly different between REM and NREM sleep (8 Hz: $P = 0.13$; 10 Hz: $P = 0.08$). Importantly, when comparing SSVEPs between presleep and postsleep wakefulness we could not reveal significant differences ($n = 18$, $P > 0.11$ for all comparisons, Fig. S5), suggesting that the observed differences between wakefulness and sleep reflect differences in state-dependent processing rather than signal instability, effects of stimulus repetition, or circadian time.

Next, we investigated the reproducibility of differences between wakefulness and sleep across participants. Wakefulness was associated with stronger SSVEPs in response to higher (8/10 Hz) frequencies, whereas both NREM and REM sleep were associated with stronger SSVEPs in response to lower (3/5 Hz) frequencies, and these effects were highly consistent in individual subject data (Fig. 3).

SSVEPs at the second harmonic were, in general, smaller in amplitude across all stimulation frequencies. However, significant differences in the second harmonic were observed at 20 Hz (in response to 10 Hz stimulation) and at 10 Hz (in response to 5 Hz stimulation). At 20 Hz, responses to 10 Hz stimulation during wakefulness ($0.05 \pm 0.01\,\mu V^2$) were significantly stronger than in NREM sleep ($0.02\,\mu V^2 \pm 0.005$, $P = 0.01$, FDR corrected) but not significantly stronger than in REM sleep ($0.02 \pm 0.007\,\mu V^2$, $P = 0.28$), while sleep states were comparable ($P = 0.37$). At 10 Hz, SSVEPs in response to 5 Hz stimulation were stronger in wakefulness ($1.41 \pm 0.92\,\mu V^2$) than in NREM sleep ($0.36 \pm 0.01\,\mu V^2$, $P = 0.05$) and REM sleep ($0.27 \pm 0.06\,\mu V^2$, $P = 0.005$, FDR corrected), but this trend did not reach statistical significance for NREM sleep due to high variability across subjects. Given the relatively small effect sizes and their high variability, we did not focus further on activity at the second harmonic in subsequent analysis.

Given that SSVEPs in wakefulness were stronger for 8/10 Hz and that spontaneous EEG alpha activity (8–12 Hz) is also prominent during wakefulness with closed eyes, we checked whether the strength of the evoked response in each participant was correlated with the magnitude of spontaneous alpha activity (Methods). We observed a statistically significant correlation between the magnitude of spontaneous alpha and the magnitude of the evoked response ($r = 0.59$, $P = 0.007$ for 8 Hz and $r = 0.4$, $P = 0.085$ for 10 Hz). However, the peak frequency of spontaneous alpha in each participant was not correlated with the frequency that drove the maximal SSVEP ($r = -0.02$, $P = 0.91$ for 8 Hz and $r = -0.21$, $P = 0.39$ for 10 Hz). No correlation was observed between evoked power in 3/5 Hz and spontaneous slow wave activity ($r = 0.29$, $P = 0.24$ for 3 Hz and $r = 0.05$, $P = 0.82$ for 5 Hz, see Methods). The relation between SSVEPs around 8/10 Hz and spontaneous alpha is discussed below.

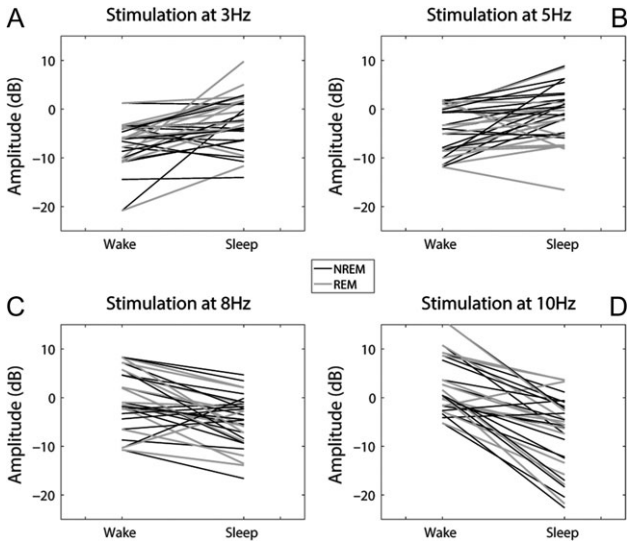

Figure 3. Differences between SSVEP responses in wakefulness and sleep are highly consistent across individual subjects. (*A–D*) SSVEP evoked power at each stimulation frequency in wakefulness (left) and in sleep (right). Gray and black lines represent paired comparisons in individual subjects between wakefulness and NREM sleep (black, $n = 19$) and wakefulness versus REM sleep (gray, $n = 10$). Note that SSVEPs to 3/5 Hz stimulation are stronger in sleep states whereas SSVEPs to 8/10 Hz are stronger in wakefulness, and these effects are highly consistent across participants.

Stronger SSVEPs During Wakefulness are Driven by More Consistent Phase Locking as Well as Higher Induced Power in Single Trials

The stronger average SSVEPs observed during wakefulness in response to 8/10 Hz and in sleep in response to 3/5 Hz stimulation could potentially reflect stronger induced power and/or more consistent phase locking at the single-trial level. Given that our data's SNR allowed single-trial analysis, we examined in detail the amplitude and phase of the occipital SSVEP in individual trials (Fig. 4) to better understand what underlies stronger SSVEP.

SSVEPs were associated with modest albeit significant induced power effects at the single-trial level, especially for 10 Hz stimulation during wakefulness. We first examined separately the power distribution in prestimulus baseline epochs and during steady-state stimulation (Methods). During baseline, analysis revealed the expected differences in activity across states with maximal energy in 3–5 Hz during NREM sleep, comparable 8 Hz energy for wakefulness and REM sleep, and maximal 10 Hz energy during wakefulness (Fig. S6, top). Power during steady-state stimulation was stronger at 3/5 Hz during sleep and stronger at 8/10 Hz during wakefulness (Fig. S6, middle). Differences between stimulation and baseline in individual trials ("induced power", Fig. 4) were stronger at 10 Hz during wakefulness (mean values: wake, NREM, REM: 15.79 ± 3.06%, 0.59 ± 0.48%, 4.24 ± 0.88%, $P < 10^{-5}$ for NREM sleep and $P = 0.02$ for REM sleep) and reached a trend for significance for 8 Hz (mean values: wake, NREM, REM: 11.29 ± 3.47%, 3.4 ± 3.6%, 4.23 ± 1.5%, $n = 19$, $P = 0.12$ for NREM and $P = 0.72$ for REM sleep). For the slow 3 Hz stimulation, induced power was significantly greater in REM sleep than wakefulness, and trended for significance for NREM sleep (mean values: wake, NREM, REM: 1.07 ± 0.99%, 4.11 ± 1.36%, 9.06 ± 3.16%, $P = 0.06$ and 0.028 for NREM and REM, respectively). We did not observe significant changes in induced power across states for 5 Hz stimulation.

SSVEPs were also associated with highly significant changes to the distribution of EEG phase at the stimulation frequency in single trials. Accordingly, phase distributions were significantly different than random across all states and frequencies (see circular plots in each upper panel, Fig. 4; Rayleigh test, $P < 10^{-11}$ in all 3 × 4 stages ∗ conditions, FDR corrected). SSVEPs in response to 8/10 Hz in wakefulness exhibited a more consistent phase distribution. Quantifying the consistency of phase distribution as PLV (also termed phase coherence, Methods), we found higher PLVs during wakefulness in response to high (8/10 Hz) frequencies (8 Hz: PLV = 0.41 ± 0.18 in wake vs. PLV = 0.14 ± 0.22 in NREM sleep, PLV = 0.21 ± 0.19 REM sleep; 10 Hz: PLV = 0.56 ± 0.15 in wake vs. PLV = 0.47 ± 0.17 in NREM sleep and PLV = 0.38 ± 0.19 REM sleep). Stronger responses to 3 Hz stimulation in sleep were also associated with more consistent phase locking (PLV = 0.46 ± 0.17 in REM sleep vs. PLV = 0.27 ± 0.2 in wake and PLV = 0.27 ± 0.2 in NREM sleep) but comparable in 5 Hz (PLV = 0.46 ± 0.17 in wake, PLV = 0.51 ± 0.17 in NREM sleep, and PLV = 0.49 ± 0.17 in REM sleep). Thus, whenever ERP results showed stronger responses in a certain state and frequency (Fig. 2), the distribution of single-trial phase values was narrower (Fig. 4). Higher phase consistency across trials

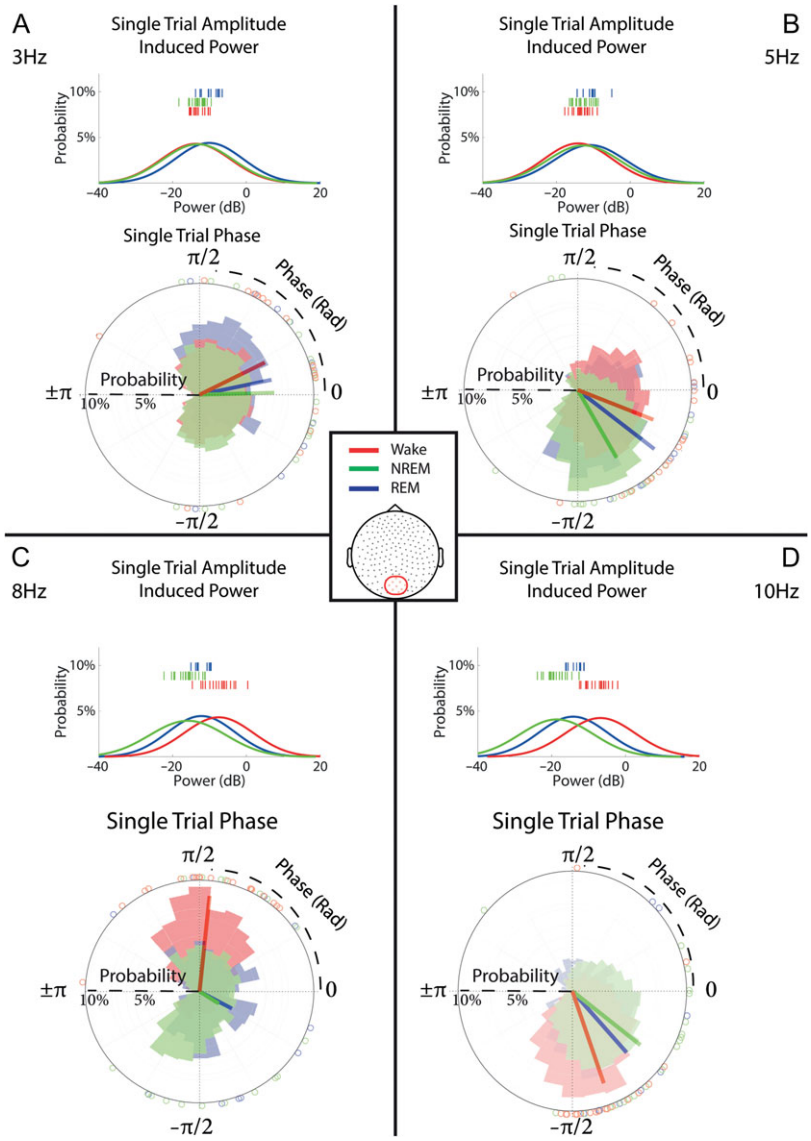

Figure 4. Distributions of EEG phase and amplitude in single-trial visual responses. (*A*) *Upper panel*: distribution of single-trial EEG amplitude values relative to prestimulus baseline ("induced power") in an occipital region of interest (middle inset) in response to visual stimulation at 3 Hz. Red, wakefulness; Green, NREM sleep; Blue, REM sleep. Power is expressed in decibels (dB, log scale). Ticks above distributions depict the average induced power effects in each participant (colors as above). *Lower panel*: distribution of single-trial EEG phase values in response to visual stimulation at 3 Hz. Shaded areas mark phase distributions (colors as above). Circles on the circle's outer perimeter depict the mean phase in individual participants. "Hand" angle shows the mean phase direction in the entire dataset, and its length represents the mean phase coherence across participants. (*B*) Same format for visual stimulation at 5 Hz. (*C*) Same format for visual stimulation at 8 Hz. (*D*) Same format for visual stimulation at 10 Hz. Note that single-trial responses to high-frequency (8/10 Hz) stimulation in wakefulness are characterized by distinct phase values (latency), higher phase consistency, and increased induced power.

was also evident when computed within individual subjects. Accordingly, higher PLV values were observed for high (8/10 Hz) frequencies during wakefulness (e.g., 8 Hz: PLV = 0.58 ± 0.06 in wake vs. PLV = 0.41 ± 0.04 in NREM sleep, $P = 0.02$; PLV = 0.36 ± 0.02 in REM sleep, $P = 0.004$; similar albeit slightly weaker effects for 10 Hz). Thus, phase consistency across trials was also apparent in single-subject data, with some of these effects reaching statistical significance after FDR correction, and others constituting a borderline trend.

In addition, SSVEPs in response to 8/10 Hz stimulation exhibited a different average phase value in wakefulness (reflecting a different response latency). Accordingly, mean phase was significantly different when comparing wakefulness to NREM sleep at high frequencies (8 Hz: 1.32 ± 0.09 rad in wake vs. −0.25 ± 0.18 rad in NREM sleep, $P = 0.002$ via random permutation test; 10 Hz: 1.03 ± 0.09 rad in wake vs. 0.47 ± 0.11 rad in NREM sleep, $P = 0.001$ via random permutation test, both FDR corrected). Effects of average phase (latency) only trended towards statistical significance at lower frequencies (3 Hz: 0.40 ± 0.13 rad in wake vs. 0.02 ± 0.13 rad in NREM sleep, $P = 0.012$ via random permutation test; 5 Hz: −0.22 ± 0.11 rad in wake vs. −0.81 ± 0.12 rad in NREM sleep, $P = 0.030$ via random permutation test, the first below the FDR threshold) but nonsignificant in REM sleep (3 Hz: 0.23 ± 0.18 rad, $P = 0.04$, 5 Hz: −0.64 ± 0.17 rad, $P = 0.26$, 8 Hz: −0.11 ± 0.20 rad, $P = 0.015$, 10 Hz: −0.65 ± 0.18 rad, $P = 0.73$, all via random permutation test in comparison to wake). Altogether, analyses of amplitude and phase effects in single trials suggest that both these factors contribute

to the enhanced ERP in response to visual flicker. In addition, responses to high-frequency stimulation in NREM sleep are associated with a different mean phase, indicating a different temporal latency of the response.

Spatio-Temporal Response Dynamics Across States

The spatio-temporal dynamics of the SSVEP were examined in more detail to better understand how wakefulness and sleep differ in their dynamics across time and scalp positions (Fig. 5). We conducted this analysis on SSVEPs in response to stimulation at all frequencies and, for the sake of brevity, present the results for 8 Hz stimulation where the maximal differences between wakefulness and sleep were observed. To this end, we averaged the response to consecutive cycles in the time domain (i.e., we treated each light pulse as a separate event), taking the time of maximal luminance as a "time-zero" for averaging (pink dotted lines, Fig. 5A). The resulting average (Fig. 5B) allowed to observe once again the stronger amplitude in the response during wakefulness, as well as the difference in phase (latency). This analysis confirmed that stronger responses to high-frequency (8/10 Hz) stimulation were typical of wakefulness, whereas stronger responses to low-frequency (3/5 Hz) stimulation were evident in both NREM and REM sleep (not shown). Furthermore, investigating the scalp topographies associated with distinct time points (Fig. 5C) revealed (1) a phase shift between the SSVEPs in wakefulness and sleep (yet similar across NREM and REM sleep), as well as (2) a highly consistent difference between topographies across states such that during wakefulness, the entire occipital cortex responded rather homogenously whereas during both NREM and REM sleep there was a robust separation between discontinuous patches across the 2 hemispheres (black arrows, Fig. 5C) and this was evident across all stimulation frequencies (not shown).

Discussion

Attenuated Fast SSVEPs During Sleep

Our paradigm effectively separated onset/offset responses from steady-state responses (Fig. 2). This separation showed that larger onset responses were a distinct feature of NREM sleep. Moreover, focusing on selective SSVEPs revealed robust differences such that SSVEPs in response to 8/10 Hz stimulation were stronger in wakefulness whereas SSVEPs in response to 3/5 Hz were stronger in sleep. Importantly, these differences were evident for both NREM and REM sleep (Fig. 2) despite substantial differences in spontaneous activity, suggesting that they

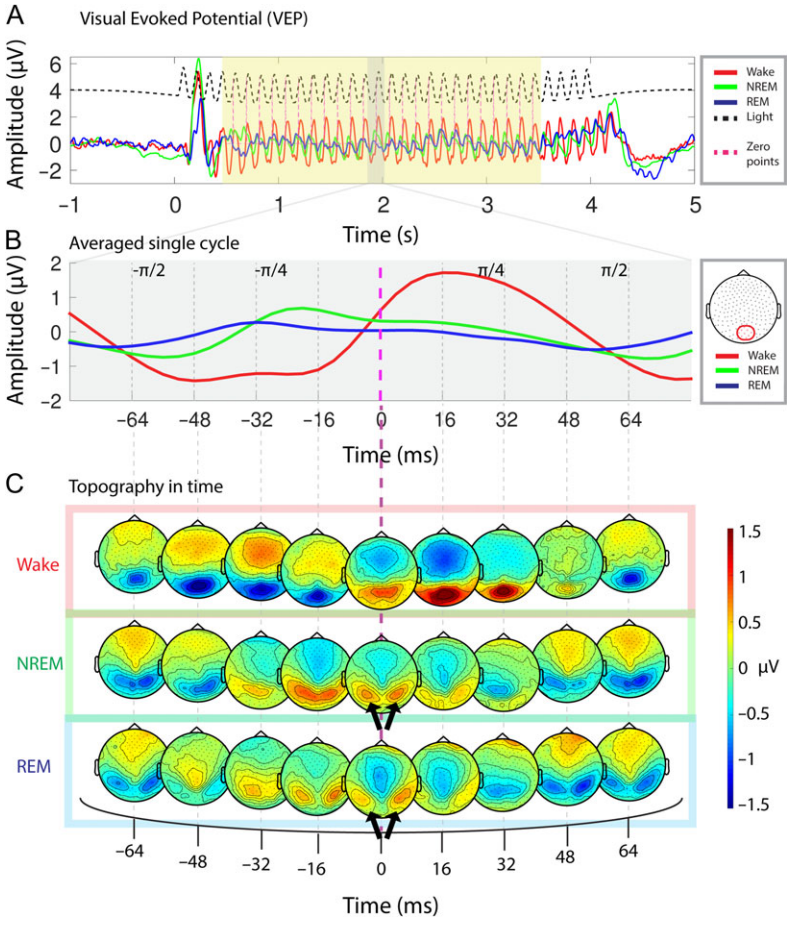

Figure 5. Visual evoked potential (VEP) waveforms and topographies. (A) Averaged VEP waveforms in response to 8 Hz visual stimulation. Solid traces: red, wake; green, NREM sleep; blue, REM sleep; dashed lines: black, light intensity recorded via photodiode; pink, time "zero" used for averaging the response across cycles in subsequent panels. (B) Average single cycle of the EEG steady-state response with respect to the pink dashed line, as seen in (A). Note increased amplitude of visual response in wakefulness. (C) Dynamics of amplitude topographies in wakefulness (top, red box), NREM sleep (middle, green box), and REM sleep (bottom, blue box). Note that NREM and REM dynamics are comparable, (both with a 2 dipoles, see black arrows) in contrast to the spatially continuous dynamics in wakefulness. See Supplementary movie 2 to view video illustrating the continuous dynamics over one luminance cycle.

capture a feature of brain activity that is associated with sensory disconnection that persists throughout sleep states. In addition, SSVEP effects were highly consistent across subjects (Fig. 3). Analyzing the separate contribution of amplitude and phase effects in individual trials (Fig. 4) revealed that stronger SSVEPs were driven by more consistent EEG phase locking and also by increased induced power at the single-trial level. In addition, NREM sleep was associated with a different mean phase value, indicating a different temporal latency in sensory responses. Finally, responses during wakefulness were homogenous across occipital cortex, whereas sleep was associated with separate discontinuous patches across the 2 hemispheres (Fig. 5).

Onset/Offset Versus Steady-State Responses

Stronger onset responses have been reported in sleep, anesthesia and drowsiness (Vanhulzen and Coenen 1984; Okusa and Kakigi 2002; Massimini et al. 2007; Riedner et al. 2011). Such onset responses may be highly similar between neuronal populations (Mak-mccully et al. 2014). Stimulus-evoked K-complexes in NREM sleep may reflect a mix of an early modality-specific component and a late nonspecific component (Riedner et al. 2011; Laurino et al. 2014), but whether specific late responses can be extracted during NREM sleep remains unclear (Perrin et al. 2000; Colrain 2005; Colrain and Campbell 2007; Laurino et al. 2014). By using steady-state stimulation, we effectively overcame this limitation, since responses consisted of an onset response, a SSVEP, and an offset response—all separated to distinct time intervals. Moreover, our stimulation method was effective in minimizing evoked K-complexes after stimulus onset (Fig. S4) that are typically abundant when applying sensory stimulation during NREM sleep (Bastien et al. 2002).

Sensory Processing Across Wakefulness and Sleep

Some previous studies reported larger/prolonged responses in sleep (Okusa and Kakigi 2002) and anesthesia (Haider et al. 2013), while others claim that responses are diminished in sleep (Livingstone and Hubel 1981) or drowsiness (Zhuang et al. 2013), with several studies pointing to cortical inhibition as a key difference (Haider et al. 2013; Zhuang et al. 2013). Conflicting results may stem from multiple experimental factors such as the receptive field occupied by the stimulus, from integrating onset/steady-state/offset components, and from stimulating at different frequencies (diverse interstimulus intervals) that we find to be affected in opposite ways by sleep. Our results reveal that sleep is associated with stronger onset responses and slow steady-state responses. In contrast, wakefulness is associated with stronger fast steady-state responses. The fact that the visual response during REM sleep, with its "wake-like" EEG, is similar to that in NREM sleep (and different than wakefulness) is of particular interest: despite strong ongoing theta activity during REM sleep (Fig. 1C) the response to 8 Hz stimulation was weak, as in NREM sleep. This highlight the importance of comparing wakefulness and REM sleep in order to contrast states of sensory incorporation (wakefulness) versus sensory disconnection (REM sleep) with similar gross electrical cortical activity (Nir et al. 2013).

Our results add to the literature comparing responses to identical sensory stimuli across wakefulness and sleep (Evarts 1963; Mukhametov and Rizzolatti 1970; Gucer 1979; Livingstone and Hubel 1981; Mariotti et al. 1989; Pena et al. 1999; Portas et al. 2000; Edeline et al. 2001; Issa and Wang 2008; Nir et al. 2015). Whether sleep primarily affects thalamocortical relay ("thalamic gating") (McCormick and Bal 1994) or intercortical connectivity (Massimini et al. 2005) remains an important open question in the field. In this context, do the SSVEPs reported here reflect early or late visual cortical activity? Although scalp EEG cannot unequivocally establish the underlying neuronal sources, the observed response topography in wakefulness (Figs 2 and 5) is typical for occipital dipoles in early visual cortex (Ossenblok and Spekreijee 1991). In addition, functional magnetic resonance imaging (fMRI) of responses evoked by identical stimuli has been localized to early visual cortex (Müller et al. 1997; Born et al. 2002; Vij et al. 2013), and neuronal activity in early visual cortex in cats and primates is highly correlated with human SSVEPs (Nakayama and Mackeben 1982; Rager and Singer 1998). Therefore, it seems plausible that the generators of the current SSVEPs may lie in early visual cortex, supporting the notion that visual processing during sleep may already be altered at this stage.

More generally, our results point to distinct spatial response profiles across states. Accordingly, analysis of response topographies revealed that across all stimulation frequencies, responses during wakefulness were more homogenous whereas responses in both NREM sleep and REM sleep had a spatially fragmented profile (Fig. 5). Such differences may reflect alterations in the topographies of spontaneous EEG in NREM and wakefulness (Brodbeck et al. 2012) and may be related to differences in response to auditory stimuli (reviewed in Colrain and Campbell 2007). It is also possible that, just like sleep increases the phase variability across trials (Fig. 4) it may also increase the phase variability across visual sub-regions, and such "phase cancellation" may lead to altered spatial topographies. Interestingly, distinct spatial signatures of sensory responses across wakefulness and sleep were reported in an fMRI study using 8 Hz visual flicker, where decreased blood oxygen level-dependent responses were found beyond primary visual areas during sleep (Born et al. 2002). Methodologies with superior spatial resolutions such as magnetoencephalography could further shed light on these intriguing spatial complexities.

Possible Underlying Mechanisms

Attenuated responses for high-frequency stimuli during anesthesia were observed in cat visual cortex (Rager and Singer 1998) and in rodent somatosensory cortex (Castro-Alamancos 2004). In humans, it was shown that auditory EEG responses during NREM sleep exhibited a similar profile as found here—with stronger responses to low-frequency stimulation in sleep and stronger responses to high-frequency stimulation during wakefulness (Tlumak et al. 2012). Castro-Alamancos (2004) proposed that sensory adaptation may be a key factor attenuating high-frequency responses to repetitive stimulation. Strong adaptation during sleep may be behaviorally advantageous since onset responses can alert a sleeping animal without subsequent detailed processing, while reduced adaptation in wakefulness can support detailed perception.

Lateral inhibition has been suggested as an explanation for intact fast SSVEPs in wakefulness, since whole-field stimulation in anesthesia are more attenuated than responses to stimuli within small receptive fields (Rager and Singer 1998). Given that scalp EEG primarily reflects synchronized postsynaptic potentials in populations of pyramidal neurons (Nunez 1981) our results suggest that during sleep, rapid synchronization of large neuronal populations at high frequencies is disrupted. While local processing within small receptive fields may

remain intact, intercortical synchronization across larger areas is impaired, reminiscent of the situation during spontaneous slow wave activity (Nir et al. 2011).

We also observed enhanced responses in NREM sleep in response to low-frequency stimulation, and this result is probably related to strong onset responses observed in NREM sleep. Indeed, low-frequency stimulation can be viewed as multiple single-trial events separated by long (200–330 ms) intervals, and may allow re-emergence of a repeated onset response.

What could be the mechanism that prevents large neuronal populations to coherently oscillate with fast stimuli during sleep? such altered responses may reflect the drastically different neuromodulatory milieu in sleep (Steriade et al. 2001). Given that attenuated fast responses were also found in REM sleep, with its activated EEG and high cholinergic tone, the key difference may stem from other modulatory systems whose activity is low throughout sleep (REM and NREM sleep) such as noradrenaline and histamine (Nir et al. 2013). Future studies should clarify if and how the presence of specific neuromodulators supports rapid synchronization among cortical populations.

What Can the Present Findings Teach Us About the SSVEP Phenomenon?

Our data confirm that 8–10 Hz constitute the optimal frequencies driving strong SSVEPs in wakefulness (Norcia et al. 2015). We found that single-trial responses to fast stimulation during wakefulness were associated with both increased induced power and with more consistent phase values (Fig. 4). Reduced phase consistency during sleep observed here joins other studies that show degraded reliability of sensory responses upon lack of attention (Kashiwase et al. 2012), reduced alertness (Zhuang et al. 2014), and anesthesia (Reinhold et al. 2015).

It has been suggested that the second harmonic better reflects higher-order attentive processing (Kim et al. 2011), but we did not find that sleep affects first and second harmonics differently, as observed in other recent studies of attention (e.g. Gray et al. 2015). Given that several studies attribute SSVEPs to specific neural oscillators that are entrained by alpha-band stimulation, our data suggest that such phase locking requires mechanisms that are specifically active during wakefulness.

Can stronger SSVEP at 8–10 Hz During Wakefulness be Explained by Alpha Activity?

SSVEPs at 8–10 Hz are often interpreted as phase entrainment of spontaneous alpha activity (Mathewson et al. 2012; Spaak et al. 2014; Notbohm et al. 2016), but see comment by Keitel et al. (2014). Could the stronger SSVEPs during wakefulness simply reflect the dominance of alpha activity during restful wakefulness? We found significant correlation between the strength of the wake SSVEP and the strength of spontaneous alpha activity in each participant, although this may simply reflect inevitable variability in data quality (with some participants showing stronger SNR for both spontaneous and stimulus-evoked activity). Our study was limited to stimulation frequencies up to 10 Hz, so it remains unknown whether stronger wake SSVEPs are specific for 8–10 Hz or whether any frequency above 5 Hz can effectively entrain EEG responses during wakefulness. Despite this limitation, several considerations suggest that the differences between wakefulness and sleep cannot be attributed in full to alpha activity during wakefulness. First and most importantly, the SSVEP in response to 8/10 Hz was significantly attenuated during REM sleep, when the EEG exhibited strong theta/alpha power (Fig. 1*D* and Fig. S6). Moreover, if the evoked responses were solely related to the spontaneous activity one would expect a correlation between the evoked low frequencies (3/5 Hz) and ongoing slow wave activity but this was not the case. Thus, SSVEPs capture information above and beyond the natural resonant frequencies of corticothalamic circuits (Rosanova et al. 2009). Second, we could not find significant correlation between the frequency of maximal SSVEP and the peak frequency of spontaneous alpha activity. Third, while the frequency of spontaneous alpha changes with age, the maximal SSVEP does not (Birca et al. 2006). Finally, SSVEPs at 15 Hz (outside the alpha range) show similar responses (Keitel et al. 2014). Altogether, it seems unlikely that stronger SSVEPs in response to 8/10 Hz stimuli during wakefulness can be explained in full by entrainment of ongoing alpha activity.

SSVEPs Through Closed Eyes as an Effective Research Tool in Unresponsive States

This work highlights the potential of SSVEPs in noninvasive human studies of sensory processing in unresponsive states. Without a task, SSVEPs have high SNRs evident in single trials (Fig. 1C), due to strong activity in visual cortex readily accessible with scalp EEG. We used full-field unstructured visual stimulation while modulating luminance at specific frequencies. In the future, stimulation can be modified along several dimensions, including other flicker frequencies, low luminance stimuli, stimulation of smaller receptive fields (e.g., left vs. right visual fields) (Gray et al. 2015), modulating color, creating apparent motion, and oddball paradigms to study hierarchical predictive coding (Strauss et al. 2015). It would be of particular interest to evoke responses in confined receptive fields and examine the brain's ability to synchronize steady-state oscillations in corresponding neuronal populations across different states.

More generally, this work demonstrates the potential utility of SSVEPs in the clinic (Vialatte et al. 2010) where it may be preferable to avoid explicit tasks, stimulate through closed eyes, and achieve robust responses in individual subjects with few trials. Indeed, attenuated SSVEPs have been reported in Parkinson's disease (Tagliati et al. 1996), migraine (Nyrke et al. 1989) and dementia (Drake et al. 1989), even when the spontaneous EEG did not show any differences. Thus, SSVEPs may constitute a more sensitive measure than analyzing ongoing activity. With future refinement, this method can be extended to other unresponsive states in which consciousness is altered such as disorders of consciousness and anesthesia (Wiedemayer et al. 2004).

Supplementary Material

Supplementary material is available at *Cerebral Cortex* online.

Funding

I-CORE Program of the Planning and Budgeting Committee and the Israel Science Foundation (Grant no. 51/11), the FP7 Marie Curie Career Integration Grant (PCIG14-GA-2013-630974), ISF grant 1326/15, and the Adelis Prize in Neuroscience.

Notes

We thank Talma Hendler for continuing support at the Tel Aviv Sourasky Medical Center; Shani Shalgi for help setting up the EEG-sleep lab; Netta Neeman for assistance with data

acquisition; Noa Bar-Ilan Regev for administrative help; Elana Zion-Golumbic and Brady Riedner for comments on earlier drafts; Issac Norman, Roy Amit, Shiri Makov, Maya Geva- Sagiv, Yaniv Sela, Amit Marmelshtein and Hagar Gelbard-Sagiv for suggestions. *Conflict of Interest*: None declared.

References

Amzica F, Steriade M. 2002. The functional significance of K-complexes. Sleep Med Rev. 6:139–149.

Bastien CH, Crowley KE, Colrain IM. 2002. Evoked potential components unique to non-REM sleep: relationship to evoked K-complexes and vertex sharp waves. Int J Psychophysiol. 46:257–274.

Bastuji H, Perrin F, Garcia-Larrea L. 2002. Semantic analysis of auditory input during sleep: studies with event related potentials. Int J Psychophysiol. 46:243–255.

Benjamini Y, Yekutieli D. 2011. The control of the false discovery rate in multiple testing under dependency source. Statistics (Ber). 29:1165–1188.

Berens P. 2009. CircStat: A MATLAB toolbox for circular statistics. J Stat Softw. 31:1–21

Birca A, Carmant L, Lortie A, Lassonde M. 2006. Interaction between the flash evoked SSVEPs and the spontaneous EEG activity in children and adults. Clin Neurophysiol. 117: 279–288.

Born AP, Law I, Lund TE, Rostrup E, Hanson LG, Wildschiødtz G, Lou HC, Paulson OB. 2002. Cortical deactivation induced by visual stimulation in human slow-wave sleep. Neuroimage. 17:1325–1335.

Brodbeck V, Kuhn A, von Wegner F, Morzelewski A, Tagliazucchi E, Borisov S, Michel CM, Laufs H. 2012. EEG microstates of wakefulness and NREM sleep. Neuroimage. 62:2129–2139.

Carskadon MA, Dement WC. 2005. Normal human sleep: an overview. Princ Pract Sleep Med. 4:13–23.

Castro-Alamancos MA. 2004. Absence of rapid sensory adaptation in neocortex during information processing states. Neuron. 41:455–464.

Cirelli C, Tononi G. 2008. Is sleep essential? PLoS Biol. 6:e216.

Colon E, Legrain V, Mouraux A. 2012. Steady-state evoked potentials to study the processing of tactile and nociceptive somatosensory input in the human brain. Neurophysiol Clin. 42:315–323.

Colrain IM. 2005. The K-complex: a 7-decade history. Sleep. 28: 255–273.

Colrain IM, Campbell KB. 2007. The use of evoked potentials in sleep research. Sleep Med Rev. 11:277–293.

Drake ME Jr, Shy KE, Liss L. 1989. Quantitation of photic driving in dementia with normal EEG. Clin Electroencephalogr. 20: 153–155.

Edeline JM, Dutrieux G, Manunta Y, Hennevin E. 2001. Diversity of receptive field changes in auditory cortex during natural sleep. Eur J Neurosci. 14:1865–1880.

Evarts EV. 1963. Photically evoked responses in visual cortex units during sleep and waking. J Neurophysiol. 26:229–248.

Galambos R, Makeig S, Talmachoff PJ. 1981. A 40-Hz auditory potential recorded from the human scalp. Proc Natl Acad Sci USA. 78:2643–2647.

Gray MJ, Frey H-P, Wilson TJ, Foxe JJ. 2015. Oscillatory recruitment of bilateral visual cortex during spatial attention to competing rhythmic inputs. J Neurosci. 35:5489–5503.

Gucer G. 1979. The effect of sleep upon the transmission of afferent activity in the somatic afferent system. Exp Brain Res. 34:287–298.

Haider B, Häusser M, Carandini M, Hausser M, Carandini M, Häusser M, Carandini M, Hausser M, Carandini M. 2013. Inhibition dominates sensory responses in the awake cortex. Nature. 493:97–100.

Harris KD, Thiele A. 2011. Cortical state and attention. Nat Rev Neurosci. 12:509–523.

Iber C, Ancoli-Israel S, Chesson A, Quan S. 2007. The AASM manual for the scoring of sleep and associated events: rules, terminology and technical specifications. 1st ed. Westchester, IL: American Academy of Sleep Medicine.

Imas OA, Ropella KM, Ward BD, Wood JD, Hudetz AG. 2005. Volatile anesthetics enhance flash-induced gamma oscillations in rat visual cortex. Anesthesiology. 102:937–947.

Issa EB, Wang X. 2008. Sensory responses during sleep in primate primary and secondary auditory cortex. J Neurosci. 28: 14467–14480.

Kakigi R, Naka D, Okusa T, Wang X, Inui K, Qiu Y, Tran TD, Miki K, Tamura Y, Nguyen TB, et al. 2003. Sensory perception during sleep in humans: a magnetoencephalograhic study. Sleep Med. 4:493–507.

Kashiwase Y, Matsumiya K, Kuriki I, Shioiri S. 2012. Time courses of attentional modulation in neural amplification and synchronization measured with steady-state visual-evoked potentials. J Cogn Neurosci. 24:1779–1793.

Keitel C, Quigley C, Ruhnau P. 2014. Stimulus-driven brain oscillations in the alpha range: entrainment of intrinsic rhythms or frequency-following response? J Neurosci. 34: 10137–10140.

Kim YJ, Grabowecky M, Paller KA, Suzuki S. 2011. Differential roles of frequency-following and frequency-doubling visual responses revealed by evoked neural harmonics. J Cogn Neurosci. 23:1875–1886.

Kouider S, Andrillon T, Barbosa LS, Goupil L, Bekinschtein TA. 2014. Inducing task-relevant responses to speech in the sleeping brain. Curr Biol. 24:2208–2214.

Landsness EC, Crupi D, Hulse BK, Peterson MJ, Huber R, Ansari H, Coen M, Cirelli C, Benca RM, Ghilardi MF, et al. 2009. Sleep-dependent improvement in visuomotor learning: a causal role for slow waves. Sleep. 32:1273–1284.

Laurino M, Menicucci D, Piarulli A, Mastorci F, Bedini R, Allegrini P, Gemignani A. 2014. Disentangling different functional roles of evoked K-complex components: mapping the sleeping brain while quenching sensory processing. Neuroimage. 86:433–445.

Livingstone MS, Hubel DH. 1981. Effects of sleep and arousal on the processing of visual information in the cat. Nature. 291: 554–561.

Llinas R, Ribary U. 1993. Coherent 40-Hz oscillation characterizes dream state in humans. Proc Natl Acad Sci USA. 90: 2078–2081.

Mak-mcCully RA, Deiss SR, Rosen BQ, Jung KY, Sejnowski TJ, Bastuji H, Rey M, Cash SS, Bazhenov M, Halgren E. 2014. Synchronization of isolated downstates (K-complexes) may be caused by cortically-induced disruption of thalamic spindling. PLoS Comput Biol. 10:e1003855.

Mariotti M, Formenti A, Mancia M. 1989. Responses of VPL thalamic neurones to peripheral stimulation in wakefulness and sleep. Neurosci Lett. 102:70–75.

Maris E, Oostenveld R. 2007. Nonparametric statistical testing of EEG- and MEG-data. J Neurosci Methods. 164:177–190.

Marshall L, Born J. 2007. The contribution of sleep to hippocampus-dependent memory consolidation. Trends Cogn Sci. 11:442–450.

Massimini M, Ferrarelli F, Esser SK, Riedner BA, Huber R, Murphy M, Peterson MJ, Tononi G. 2007. Triggering sleep slow waves by transcranial magnetic stimulation. Proc Natl Acad Sci USA. 104:8496–8501.

Massimini M, Ferrarelli F, Huber R, Esser SK, Singh H, Tononi G. 2005. Breakdown of cortical effective connectivity during sleep. Science. 309:2228–2232.

Mathewson KE, Prudhomme C, Fabiani M, Beck DM, Lleras A, Gratton G. 2012. Making waves in the stream of consciousness: entraining oscillations in EEG alpha and fluctuations in visual awareness with rhythmic visual stimulation. J Cogn Neurosci. 24:2321–2333.

McCormick DA, Bal T. 1994. Sensory gating mechanisms of the thalamus. Curr Opin Neurobiol. 4:550–556.

McDonald DG, Schicht WW, Frazier RE, Shallenberger HD, Edwards DJ. 1975. Studies of information processing in sleep. Psychophysiology. 12:624–629.

Mukhametov LM, Rizzolatti G. 1970. The responses of lateral geniculate neurons to flashes of light during the sleep-waking cycle. Arch Ital Biol. 108:348–368.

Mukhametov LM, Supin AY, Polyakova IG. 1977. Interhemispheric asymmetry of the electroencephalographic sleep patterns in dolphins. Brain Res. 134:581–584.

Müller MM, Teder W, Hillyard SA. 1997. Magnetoencephalographic recording of steady-state visual evoked cortical activity. Brain Topogr. 9:163–168.

Nakayama KEN, Mackeben M. 1982. Steady state visual evoked potentials in the alert primate. Vision Res. 22:1261–1271.

Nir Y, Massimini M, Boly M, Tononi G. 2013. Sleep and consciousness. In: Cavanna AE, Nani A, Blumenfeld H, Laureys S, editors. Neuroimaging of consciousness. Springer Berlin Heidelberg. p. 133–182.

Nir Y, Staba RJ, Andrillon T, Vyazovskiy V V, Cirelli C, Fried I, Tononi G. 2011. Regional slow waves and spindles in human sleep. Neuron. 70:153–169.

Nir Y, Tononi G. 2010. Dreaming and the brain: from phenomenology to neurophysiology. Trends Cogn Sci. 14:88–100.

Nir Y, Vyazovskiy V V, Cirelli C, Banks MI, Tononi G. 2015. Auditory responses and stimulus-specific adaptation in rat auditory cortex are preserved across NREM and REM sleep. Cereb Cortex. 25:1362–1378.

Norcia AM, Appelbaum LG, Ales JM, Cottereau BR, Rossion B. 2015. The steady-state visual evoked potential in vision research : a review. J Vis. 15:1–46.

Notbohm A, Kurths J, Herrmann CS. 2016. Modification of Brain Oscillations via Rhythmic Light Stimulation Provides Evidence for Entrainment but Not for Superposition of Event-Related Responses. Front Hum Neurosci. 10:10.

Nunez PL. 1981. Electric fields of the brain: the neurophysics of EEG. New York: Oxford University Press.

Nyrke T, Kangasniemi P, Lang AH. 1989. Difference of steady-state visual evoked potentials in classic and common migraine. Electroencephalogr Clin Neurophysiol. 73:285–294.

Okusa T, Kakigi R. 2002. Structure of visual evoked magnetic field during sleep in humans. Neurosci Lett. 328:113–116.

Oostenveld R, Fries P, Maris E, Schoffelen JM. 2011. FieldTrip: open source software for advanced analysis of MEG, EEG, and Invasive Electrophysiological Data. Comput Intell Neurosci. 2011:1–9.

Ossenblok P, Spekreijee H. 1991. The extrastriate generators of the EP to checkerboard onset. A source localization approach. Electroencephalogr Clin Neurophysiol Potentials Sect. 80: 181–193.

Oswald I, Taylor AM, Treisman M. 1960. Discriminative responses to stimulation during human sleep. Brain. 83: 440–453.

Pena JL, Perez-Perera L, Bouvier M, Velluti RA. 1999. Sleep and wakefulness modulation of the neuronal firing in the auditory cortex of the guinea pig. Brain Res. 816:463–470.

Perrin F, Bastuji H, Mauguière F, García-Larrea L. 2000. Functional dissociation of the early and late portions of human K-complexes. Neuroreport. 11:1637–1640.

Pigarev IN, Fedorov GO, Levichkina E V, Marimon JM, Pigareva ML, Almirall H. 2011. Visually triggered K-complexes: a study in New Zealand rabbits. Exp Brain Res. 210:131–142.

Plourde G. 2006. Auditory evoked potentials. Best Pr Res Clin Anaesthesiol. 20:129–139.

Portas CM, Krakow K, Allen P, Josephs O, Armony JL, Frith CD. 2000. Auditory processing across the sleep-wake cycle: simultaneous EEG and fMRI monitoring in humans. Neuron. 28: 991–999.

Rager G, Singer W. 1998. The response of cat visual cortex to flicker stimuli of variable frequency. Eur J Neurosci. 10: 1856–1877.

Regan D. 1966. Some characteristics of average steady-state and transient responses evoked by modulated light. Electroencephalogr Clin Neurophysiol. 20:238–248.

Reinhold K, Lien AD, Scanziani M. 2015. Distinct recurrent versus afferent dynamics in cortical visual processing. Nat Neurosci. 18:1789–1797.

Riedner BA, Hulse BK, Murphy MJ, Ferrarelli F, Tononi G. 2011. Temporal dynamics of cortical sources underlying spontaneous and peripherally evoked slow waves. Prog Brain Res. 193:201–218.

Riedner BA, Vyazovskiy V V, Huber R, Massimini M, Esser S, Murphy M, Tononi G. 2007. Sleep homeostasis and cortical synchronization: III. A high-density EEG study of sleep slow waves in humans. Sleep. 30:1643–1657.

Rosanova M, Casali A, Bellina V, Resta F, Mariotti M, Massimini M. 2009. Natural frequencies of human corticothalamic circuits. J Neurosci. 29:7679–7685.

Spaak E, de Lange FP, Jensen O. 2014. Local entrainment of alpha oscillations by visual stimuli causes cyclic modulation of perception. J Neurosci. 34:3536–3544.

Steriade M, McCormick DA, Sejnowski TJ. 1993. Thalamocortical oscillations in the sleeping and aroused brain. Science. 262: 679–685.

Steriade M, Timofeev I, Grenier F. 2001. Natural waking and sleep states: a view from inside neocortical neurons. J Neurophysiol. 85:1969–1985.

Strauss M, Sitt JD, King JR, Elbaz M, Azizi L, Buiatti M, Naccache L, van Wassenhove V, Dehaene S. 2015. Disruption of hierarchical predictive coding during sleep. Proc Natl Acad Sci USA. 112:E1353–E1362.

Tagliati M, Bodis-Wollner I, Yahr MD. 1996. The pattern electroretinogram in Parkinson's disease reveals lack of retinal spatial tuning. Electroencephalogr Clin Neurophysiol. 100:1–11.

Tlumak AI, Durrant JD, Delgado RE, Boston JR. 2012. Steady-state analysis of auditory evoked potentials over a wide range of stimulus repetition rates in awake vs. natural sleep. Int J Audiol. 51:418–423.

Tononi G, Cirelli C. 2014. Sleep and the price of plasticity: from synaptic and cellular homeostasis to memory consolidation and integration. Neuron. 81:12–34.

Vanhulzen Z, Coenen A. 1984. Photically evoked potentials in the visual cortex following paradoxical sleep deprivation in rats. Physiol Behav. 32:557–563.

Vialatte FB, Maurice M, Dauwels J, Cichocki A. 2010. Steady-state visually evoked potentials: focus on essential paradigms and future perspectives. Prog Neurobiol. 90: 418–438.

Vij N, Zuobin W, Bjoernsdotter M, Dauwels J, Vialatte FB. 2013. A multimodal approach to analysis of steady state visually evoked potentials. Proc 2013 IEEE Symp Comput Intell Bioinforma Comput Biol. p. 183–188.

Wiedemayer H, Fauser B, Sandalcioglu IE, Armbruster W, Stolke D, Armbruster A, Stolke D. 2004. Observations on intraoperative monitoring of visual pathways using steady-state visual evoked potentials. Eur J Anaesthesiol. 21:429–433.

Xie L, Kang H, Xu Q, Chen MJ, Liao Y, Thiyagarajan M, O'Donnell J, Christensen DJ, Nicholson C, Iliff JJ, et al. 2013. Sleep drives metabolite clearance from the adult brain. Science. 342:373–377.

Zhuang J, Bereshpolova Y, Stoelzel CR, Huff JM, Hei X, Alonso JM, Swadlow HA. 2014. Brain state effects on layer 4 of the awake visual cortex. J Neurosci. 34:3888–3900.

Zhuang J, Stoelzel CR, Bereshpolova Y, Huff JM, Hei X, Alonso JM, Swadlow HA. 2013. Layer 4 in primary visual cortex of the awake rabbit: contrasting properties of simple cells and putative feedforward inhibitory interneurons. J Neurosci. 33: 11372–11389.